VOL. 12, NO. 14, JULY 2017 ISSN 1819-6608

ARPN Journal of Engineering and Applied Sciences

www.arpnjournals.com

MODEL VALIDATION FOR FLOW AND HEAT TRANSFER CHARACTERISTICS OF SUPERCRITICAL CO_2 IN MINI-CHANNELS

N. T. Rao, A. N. Oumera, U. K Jamaludina, Hassan Ibrahima, Firdaus Basrawia and A. Y. Adama
Faculty of Mechanical Engineering, Universiti Malaysia Pahang, Pahang, Malaysia
E-Mail: thiwaan@hotmail.com

ABSTRACT

Carbon dioxide (CO_2) at supercritical phase is being used recently in Heating, Ventilation, Air Conditioning and Refrigeration (HVAC&R) industries due to its special thermal properties of supercritical CO_2, which leads to better performance of heat transfer and flow characteristics. Therefore, the main purpose of this study is to develop flow and heat transfer CFD models and validate the models by comparing with previous studies from literature. For the simulation, the CO_2 flow was assumed to be incompressible, turbulent, non-isothermal and Newtonian. The numerical results compared with the experimental data obtained from (Liao and Zhao 2002). The experimental data consisted of three different cases with different inlet pressure (P), inlet temperature (Tin) and tube diameter (d). All the maximum and minimum temperature percentage differences for all three cases are in a small values. Moreover, the surface area, A of the tube is inversely proportional to heat transfer coefficient (h). Besides, the pressure drop (ΔP) for all three cases increased together with h when the tube diameters decreased. The numerical results were in good agreement with experimental results for temperature distributions. The CFD model is validated.

Keywords: CO_2, CFD, supercritical phase, heat transfer, pressure drop, validation.

INTRODUCTION

Carbon dioxide (CO_2) gas has zero global warming potential (GWP) and ozone depleting potential (ODP). Hence, it was reintroduced as an environmental friendly gas, and used as working fluid in refrigerators and air conditioning systems. Besides, CO_2 gas is non-toxic and safe to humans, abundant and non-combustible. Meanwhile, at supercritical phase, CO_2 reaches near to its critical point, the physical properties shows extremely rapid variations with a change in temperature and pressure (Bolaji and Huan 2013). Hence, CO_2 with the special thermo-fluid properties and appropriate design, at supercritical phase, makes it the ideal replacement for chlorofluorocarbons (CFCs) and hydrochlorofluoro-carbons (HCFCs).

Moreover, supercritical CO_2 undergo significant changes in the density and dynamic viscosity of CO_2 at supercritical phase, which is almost vertical within a very narrow temperature range while the enthalpy undergoes a sharp increase near the critical point (Liao and Zhao 2002). As the temperature of supercritical CO_2 flowing in the tube increases in near-critical region, the pressure drop and heat transfer coefficient are increased too (Huai *et al.* 2005). At larger Reynolds number, heat transfer coefficient increased as the heat transfer rate increased (Hsieh *et al.* 2014). Even though a few researchers had performed studies and investigation on cooling heat transfer and flow of supercritical CO_2 in mini-channels, it still appears an unsolved issue. The density (ρ), thermal conductivity (λ), viscosity (μ) and specific heat (C_p) of supercritical CO_2 vary at different pressure and temperature values (Lemmon *et al.* 2015).

Most of the researchers have studied the flow and heat transfer characteristics of supercritical CO_2 by using experimental methods. However, few research work using numerical and analytical methods have also been documented. The geometry often used for mathematical model is the circular tube-in-tube heat exchanger, where supercritical CO_2 flows in the inner tube and cooling water flow in the annular space. A few numerical analysis are done by using Renormalization Group (RNG) k-ε and Low-Reynolds number (LRN) k-ε models as the turbulence model with ANSYS FLUENT CFD codes (Xu *et al.* 2015; Mohseni and Bazargan 2012; Lisboa *et al.* 2010; Yadav *et al.* 2014). Besides, the flow domains are divided into two; CO_2 and water for cooling process (Yadav *et al.* 2012; Jiang *et al.* 2009).

The main purpose of this study is to develop flow and heat transfer CFD models and validate the models by comparing with previous studies from literature. This study is expected to provide better knowledge on enhancing the heat transfer and flow characteristics on CO_2.

MATHEMATICAL FORMULATIONS

Governing equations

In this study, the flow field is assumed to be incompressible, steady, non-isothermal and two-dimensional (2D) flow. Therefore, the governing equations for the continuity, momentum and energy can be expressed as (Cengel and Cimbala 2013):

Continuity equation:

$$\vec{\nabla} \cdot \vec{V} = 0 \tag{1}$$

where $\vec{V}$ is the velocity vector and $\vec{\nabla}$ is divergence operator.

Momentum equation:

$$\rho \frac{D\vec{V}}{Dt} = \rho \left[\frac{\partial \vec{V}}{\partial t} + \left(\vec{\nabla} \cdot \vec{V}\right)\vec{V}\right] = -\vec{\nabla}P + \rho\vec{g} + \mu\vec{\nabla}^2\vec{V} \tag{2}$$

where ρ is density of the fluid (kg/m^3), t is time (seconds), g is gravitational acceleration (m/s^2) andμ in the fluid viscosity (kg/m.s)

Conservation of energy equation:

$$\rho C_P \left(\frac{\partial T}{\partial t} + \vec{V} \cdot \vec{\nabla}T\right) = k\vec{\nabla}^2 T + \dot{\gamma} \cdot \tau \tag{3}$$

where, P is the hydrostatic pressure (Pa), C_p is the specific heat (J/kg.K), and k is the thermal conductivity (W/m.K). The term $\dot{\gamma}$ represents the shear rate,$\tau$is the total stress tensor.

Pressure drop equations

Pressure drop (ΔP) takes place due to pressure loss in a system due to friction in the system. The ΔP equation represents the relationship between friction factor, length to diameter of tube ratio, and density and velocity of the fluid. The general equation of ΔP is:

$$\Delta P = f.\frac{L}{D}.\frac{\rho V^2}{2} \tag{4}$$

where f is friction factor, L is length of the tube (m) and D is diameter of the tube (m). The friction factor for equation (4) will be calculated with Reynolds number obtained from equation (5). For turbulent flow, Colebrook equation was used to calculate friction factor:

$$\frac{1}{\sqrt{f}} = -2.0 \log\left(\frac{\varepsilon D}{3.7} + \frac{2.51}{Re\sqrt{f}}\right) \tag{5}$$

where ε is pipe roughness.

Heat transfer rate equations

Heat transfer rate was expressed by using following equation (Liao and Zhao 2002; Cengel and Ghajar 2011):

$$\dot{Q} = \dot{m}C_p(T_{in} - T_{out}) \tag{6}$$

Where $\dot{Q}$ is heat transfer rate (W), $\dot{m}$ is mass flow rate (kg/s), C_P is specific heat at constant pressure (J/kg.^{o}C), and T_{in} and T_{out} are the inlet and outlet temperatures of fluid (ºC), respectively. Besides, the logarithmic mean temperature difference (LMTD) by using average inner wall temperature, $T_w$was calculated as (Adams *et al*. 1997):

$$LMTD = \frac{(T_{in}-T_W)-(T_{out}-T_W)}{\ln\left(\frac{T_{in}-T_W}{T_{out}-T_W}\right)} \tag{7}$$

The average heat transfer coefficient, h along the cooling length was calculated using the following equation:

$$h = \frac{\dot{Q}}{A*LMTD} \tag{8}$$

where h is heat transfer coefficient (W/m^2.ºC) and A is inner surface area of the tube (m^2).

NUMERICAL ANALYSIS

Computational domain

Design Modeler software was used to design the flow domains. It was designed according to the tube-in-tube heat exchanger: CO_2 and water flow domains, with stainless steel tube between them. The diameter of the inner tube and cooling length was decided to be in line with the experimental set up from Liao and Zhao (Liao and Zhao 2002), as stated in Table-1. Due to symmetry of the tubes, only half of the model is considered in this study and the 2D schematic of the tube-in-tube heat exchanger model as shown in Figure-1.

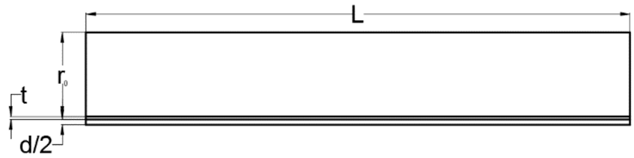

Figure-1. 2D tube-in-tube heat exchanger design in design modeler.

Table-1. Dimensions of flow domain.

Case	Tube inner diameter, *d* (mm)	Cooling length, *L* (mm)
1	2.16	110
2	1.40	110
3	0.70	110

As shown in Figure-1, L is the total cooling length, $d/2$ is the radius of the inner tube, t is thickness of the inner tube and r_0 is height of outer tube. As mentioned earlier, the fluids used for the numerical analysis are water as the cooling fluid and CO_2 as the operating fluid. The thermophysical properties of CO_2 available in ANSYS FLUENT database are only at room temperature. Therefore, the thermophysical process of CO_2 at supercritical phase were taken from National Institute of Standards and Technology (NIST) web book (Lemmon *et al*. 2015) and included in ANSYS FLUENT database. The thermophysical properties of CO_2 for all three cases were obtained according to the inlet pressures and inlet temperatures, and are tabulated in Table-2.

VOL. 12, NO. 14, JULY 2017 ISSN 1819-6608
ARPN Journal of Engineering and Applied Sciences

Table-2. Thermophysical properties of CO_2 for all three cases (Lemmon *et al*. 2015).

Case	Inlet pressure, P (MPa)	Inlet temperature T_{in} (°C)	Density, ρ (kg/m³)	Thermal conductivity, λ (W/m.K)	Viscosity, μ (Pa.s)	Specific heat, C_p (J/g.K)
1	7.953	66.7	177.30	0.028639	0.000019904	1.7194
2	10.044	31.8	753.42	0.082442	0.000063337	3.4429
3	7.929	51.1	211.70	0.031481	0.000020268	2.3659

Meshing

The mesh size is setup to be fine. The mesh control tools such as mesh sizing and mapped face meshing were used to create finer mesh sizes with proper arrangement. Moreover, mesh independent test was conducted to make sure that the numerical analysis results are same for all mesh sizes. The optimum number of mesh size for the simulation was 100,068.

Boundary conditions

For this study, the $CO_2$was assumed as incompressible flow for both vapor and supercritical phases. The CO_2 and water flow in the inner tube and outer tube respectively. The boundary conditions of CO_2 were obtained from previous study (Liao and Zhao 2002) and used in the numerical analysis, as tabulated in Table-3. The supercritical CO_2 inlet static pressures used were 7.953 MPa, 10.044 MPa and 7.929 MPa, and the inlet mass flow rate inlet for all three static pressures was 0.0005 kg/s. Meanwhile, for water domain, the mass flow rate inlet was 0.005 kg/s with inlet temperature of 27 °C.

Table-3. Boundary conditions for supercritical CO_2.

Case	Inlet pressure, P (MPa)	Inlet temperature T_{in} (°C)	Outlet temperature T_{out} (°C)
1	7.953	66.7	42.4
2	10.044	31.8	25.4
3	7.929	51.1	48.0

From the numerical analysis, the temperature distributions, heat transfer coefficient and pressure drop were obtained from data collected through total pressures, outer and inner wall static temperatures, and surface heat transfer coefficients. These data were analyzed and compared with the experimental data from Liao and Zhao (Liao and Zhao 2002). Then, the temperature, heat transfer coefficients, and pressure drop were determined.

Temperature distributions

Shown in Figure-2 is the comparison between experimental results from previous study and the current numerical results. The numerical results were taken at six different positions along the tube length. As can be clearly seen from Figure-2, results for all cases were in good agreement with the experimental results, with maximum difference of 2 °C.

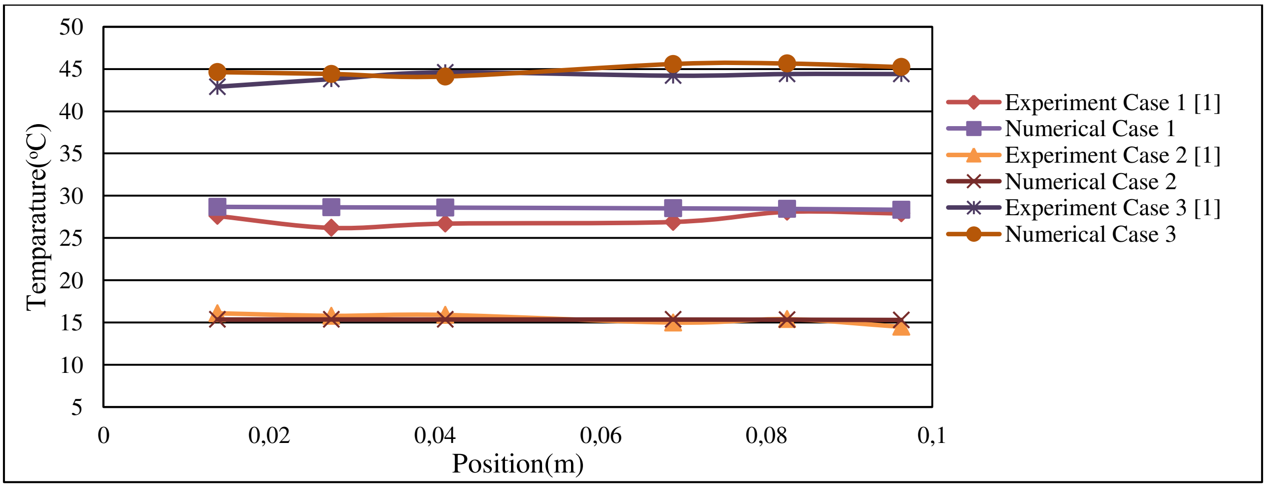

Figure-2. Comparison between experimental and numerical results for temperature distribution of all three cases.

ARPN Journal of Engineering and Applied Sciences

For Case 1, the experimental supercritical CO_2 temperature decreased from 0.01375 m position to 0.0275 m position. Then it rose back to the highest value, 28.1 ^oC at 0.0835 m position and later decreased again as it approaches the outlet. On the other hand, for the numerical results, the temperature decreased continuously, but slowly, from 28.688 ^oC at inlet to 28.344 ^oC at outlet of the pipe. The maximum and minimum temperature differences between experimental and numerical results for Case 1 were 9.3% and 1.2% respectively. Furthermore, for case 2, both experimental and numerical temperature distribution results decreased along the tube length. The maximum and minimum temperature differences between experimental and numerical results for Case 2 were 5.6% and 0.4% respectively. Meanwhile, for Case 3 experimental results, the temperature increased slowly from first until third position. Then, it decreased and increased again at fourth and fifth positions, respectively, and became constant. However, the temperature decreased from first until third position, increased up to fifth position and finally decreased again. The maximum and minimum temperature differences between experimental and numerical results for Case 3 is 4% and 1.1% respectively. All the maximum and minimum differences for all three cases are in a small values. Due to this reason, the heat transfer models are valid.

Heat transfer

The average heat transfer coefficient (h) results were obtained from the numerical results for all three cases. Figure-3 shows the comparison between calculated h and h from numerical results. The h was calculated by using Equation. (6), Equation. (7) and Equation. (8). For Case 1, the h from value from numerical results was 5.8% higher than experimental h. Meanwhile, for Case 2, the experimental h was 0.8% higher than the numerical results h. Case 1 and Case 2 shown small value in percentage difference. Moreover, for Case 3, the numerical h was 20% higher than the experimental h. All the percentage differences for all three cases are in a small values. Due to this reason, the heat transfer models are valid.

Meanwhile, as the $h$is related to the tube diameter, d in Table-4, the value of h increased when the d is decreased. This is because the surface area, A of the tube is inversely proportional to heat transfer coefficient, h, refer Equation. (8)

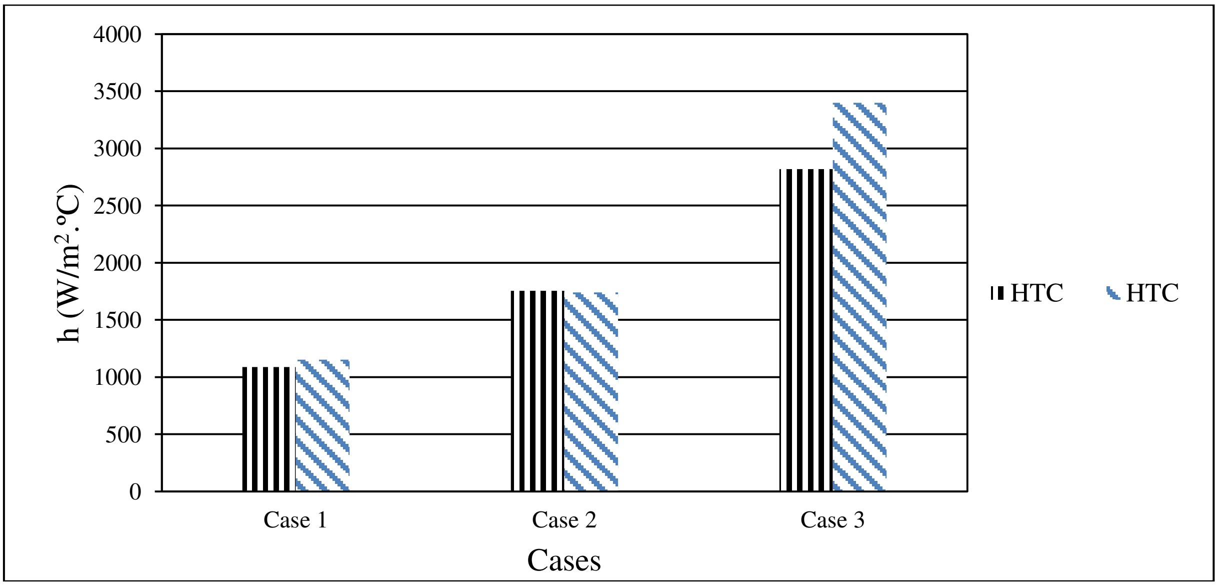

Figure-3. Calculated and simulated average heat transfer coefficient comparison for all three cases.

Pressure drop

The total pressure drop (ΔP) data were not stated in the previous studies (Liao and Zhao 2002). Hence, Table-4 shows the relationship between total ΔP from numerical analysis with inlet temperatures, inlet pressures and tube diameters for all three cases.

As shown in Table-4, the ΔP increased as the tube diameter decreased. The ΔP value was the highest for Case 3 when the tube diameter is small and the inlet pressure in near critical point (P_{cr}= 7.39 MPa). According to (Chen *et al*. 2013), when the inlet pressure, P increased, the ΔP decreases. This statement verifies the Δ $P$of Case 2 and Case 3. Besides, Hiesh (Hsieh *et al*. 2014) proved that heat transfer coefficient, h increased with Reynolds number (Re). In the other hand, ΔP also increased with Re. From section 4.2, the A of the tube is inversely proportional to h. Hence, ΔP is considered increased when the tube diameter, d decreases.

ARPN Journal of Engineering and Applied Sciences

Table-4. Effect of boundary conditions on pressure drop for all three cases.

Case	Inlet pressure, *P* (MPa)	Inlet temperature T_{in} (°C)	Tube diameter, *d* (mm)	Pressure drop, ΔP (Pa)
1	7.953	66.7	2.16	290.70
2	10.044	31.8	1.40	815.98
3	7.929	51.1	0.70	14492.37

CONCLUSIONS

In this study, the flow and heat transfer CFD models were developed and validated by comparing with the previous studies from literature (Liao and Zhao 2002). For the temperature distributions of all three cases for numerical results were in good agreement with the experimental results, with maximum difference of 2°C. The temperature distributions from numerical results for all three cases decrease slightly as the supercritical CO_2 flows through the tube. All the maximum and minimum temperature differences for all three cases are in a small values. Meanwhile, both experimental and numerical results on average heat transfer coefficient increases as the tube diameter decreases. The surface area, *A* of the tube is inversely proportional to heat transfer coefficient, *h*. All the percentage differences of *h* for all three cases are in a small values. Due to this reasons, the heat transfer models are valid.

For Case 2 and Case 3, when the inlet pressure, *P* increased, the ΔP decreases. However, the pressure drop (ΔP) for all three cases increased together with *h* when the tube diameters decreased. The numerical results were in good agreement with experimental results for temperature distributions. The CFD model is validated.

ACKNOWLEDGEMENT

The authors would like to be thanking Universiti Malaysia Pahang for providing laboratory facilities and Ministry of Higher Education Malaysia for financial assistance under FRGS project no. RDU130132.

REFERENCES

S. M. Liao and T. S. Zhao, "Measurements of Heat Transfer Coefficients From Supercritical Carbon Dioxide Flowing in Horizontal Mini/Micro Channels," Journal of Heat Transfer, vol. 124, pp. 413-420, 2002.

B. O. Bolaji and Z. Huan, "Ozone depletion and global warming: Case for the use of natural refrigerant - a review," Renewable and Sustainable Energy Reviews`, vol. 18, pp. 49-54, 2013.

S. M. Liao and T. S. Zhao, "An experimental investigation of convection heat transfer to supercritical carbon dioxide in miniature tubes," International Journal of Heat and Mass Transfer, vol. 45, pp. 5025-5034, 2002.

X. L. Huai, S. Koyama, and T. S. Zhao, "An experimental study of flow and heat transfer of supercritical carbon dioxide in multi-port channels under cooling conditions," Chemical Engineering Science, vol. 60, pp. 3337-3345, 2005.

J. C. Hsieh, B. H. Lee, M. C. Chung, D. T. W. Lin, and S. H. Guo, "Experimental study of heat transfer for supercritical carbon dioxide with upward flow in vertical tube," International Journal of Advanced Science and Technology, vol. 7, pp. 66-71, 2014.

E. W. Lemmon, M. O. McLinden, and D. G. Friend. 2015. "Thermophysical Properties of Fluid Systems" in NIST Chemistry WebBook, NIST Standard Reference Database Number 69, Eds. P.J. Linstrom and W.G. Mallard. Available: http://webbook.nist.gov

J. Xu, C. Yang, W. Zhang, and D. Sun, "Turbulent convective heat transfer of CO_2 in a helical tube at near-critical pressure," International Journal of Heat and Mass Transfer, vol. 80, pp. 748-758, 2015.

M. Mohseni and M. Bazargan, "Modification of low Reynolds number k-e turbulence models for applications in supercritical fluid flows," International Journal of Thermal Sciences, vol. 51, pp. 51-62, 2012.

P. F. Lisboa, J. Fernandes, P. C. Simoes, J. P. B. Mota, and E. Saatdjian, "Computational-fluid-dynamics study of a Kenics static mixer as a heat exchanger for supercritical carbon dioxide," Journal of Supercritical Fluids, vol. 55, pp. 107-155, 2010.

A. K. Yadav, M. R. Gopal, and S. Bhattacharyya, "Transient analysis of subcritical/supercritical carbon dioxide based natural circulation loops with end heat exchangers: Numerical studies," International Journal of Heat and Mass Transfer, vol. 79, pp. 24-33, 2014.

K. Yadav, M. R. Gopal, and S. Bhattacharyya, "CFD analysis of a CO_2 based natural circulation loop with end heat exchangers," Applied Thermal Engineering, vol. 36, pp. 288-295, 2012.

P. X. Jiang, C. R. Zhao, R. F. Shi, Y. Chen, and W. Ambrosini, "Experimental and numerical study of convection heat transfer of CO_2 at super-critical pressures during cooling in small vertical tube," International Journal of Heat and Mass Transfer, vol. 52, pp. 4748-4756, 2009.

Y. A. Cengel and J. M. Cimbala, Fluid Mechanics: Fundamentals and Applications. New York: McGraw-Hill, 2013.

Y. A. Cengel and A. J. Ghajar, Heat and Mass Transfer: Fundamentals and Applications, 4th Edition ed. New York: McGraw-Hill Higher Education, 2011.

T. M. Adams, S. I. A. Khalik, S. M. Jeter, and Z. H. Qureshi, "An experimental investigation of single-phase forced convection in microchannels," International Journal of Heat and Mass Transfer, vol. 41, pp. 851-857, 1997.

L. Chen, B. L. Deng, B. Jiang, and X. R. Zhang, "Thermal and hydrodynamic characteristics of supercritical CO2 natural circulation in closed loops," Nuclear Engineering and Design, vol. 257, pp. 21-30, 2013.